ACS OMEGA

Open Access

http://pubs.acs.org/journal/acsodf

Article

Quantitative Proteomics Reveal the Role of Matrine in Regulating Lipid Metabolism

Huixu Feng, Guobin Liu, Luhan Li, Xuelian Ren, Yue Jiang, Wanting Hou, Ruilong Liu, Kun Liu, Hong Liu, and He Huang*

Cite This: *ACS Omega* 2024, 9, 24308−24320

Read Online

ACCESS | Metrics & More | Article Recommendations | Supporting Information

ABSTRACT: Hyperlipidemia (HLP) is a prevalent systemic metabolic disorder characterized by disrupted lipid metabolism. Statin drugs have long been the primary choice for managing lipid levels, but intolerance issues have prompted the search for alternative treatments. Matrine, a compound derived from the traditional Chinese medicine Kushen, exhibits anti-inflammatory and lipid-lowering properties. Nevertheless, the mechanism by which matrine modulates lipid metabolism remains poorly understood. Here, we investigated the molecular mechanisms underlying matrine's regulation of lipid metabolism. Employing quantitative proteomics, we discovered that matrine increases the expression of LDL receptor (LDLR) in HepG2 and A549 cells, with subsequent experiments validating its role in enhancing LDL uptake. Notably, in hyperlipidemic hamsters, matrine effectively lowered lipid levels without affecting body weight, which highlights LDLR as a critical target for matrine's impact on HLP. Moreover, matrine's potential inhibitory effects on tumor cell LDL uptake hint at broader applications in cancer research. Additionally, thermal proteome profiling analysis identified lipid metabolism-related proteins that may interact with matrine. Together, our study reveals matrine's capacity to upregulate LDLR expression and highlights its potential in treating HLP. These findings offer insights into matrine's mechanism of action and open new avenues for drug research and lipid metabolism regulation.

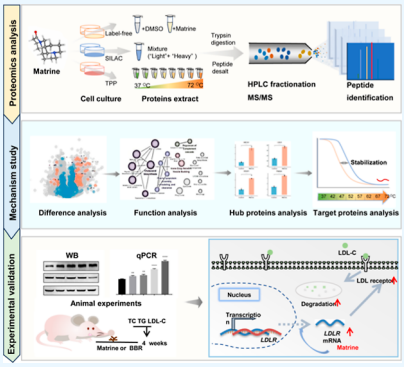

INTRODUCTION

Hyperlipidemia (HLP) is a prevalent systemic metabolic disorder characterized by dysregulated lipid metabolism, resulting in elevated levels of total cholesterol (TC), triglyceride (TG), and low-density lipoprotein cholesterol (LDL-C) in circulation.[1,2] This perturbation in lipid metabolism contributes to the progression of atherosclerosis and can lead to cardiovascular diseases (CVDs).[3] As a consequence, HLP is recognized as a significant risk factor for CVDs.[4] Furthermore, lipid accumulation can trigger common complications such as thrombus-induced myocardial infarction (MI) and stroke,[3,5,6] underscoring the urgency for early intervention in HLP.

Across the past few decades, diverse lipid-lowering medications have been developed, with statins being a representative example. Statins function by inhibiting intracellular cholesterol synthesis, leading to an elevation in the expression of low-density lipoprotein receptor (LDLR) and aiding in the maintenance of plasma cholesterol levels via LDL-C endocytosis. However, a subset of patients experience intolerance to statin treatments.[7] Therefore, the exploration of nonstatin lipid-lowering alternatives assumes significance.[8,9]

Natural products represent a significant reservoir of potential drug candidates, owing to their distinctive strengths, such as chemical diversity, biological activity, and so on. Consequently, the discovery and development of novel natural products have become an important area of research in anti-HLP treatments.[10,11] Kushen, derived from the roots of *Sophora flavescens*, a well-known traditional Chinese medicine belonging to the leguminous family, is indigenous to China, India, Japan, Korea, and Russia.[12] Historically, the dried roots of Kushen have been utilized for addressing various health issues, including tumors and inflammation.[13] Kushen contains diverse alkaloid compounds including matrine (molecular formula: $C_{15}H_{24}N_2O$, molecular weight: 248.36 g/mol), oxymatrine, and sophorine.[13,14] Recent studies have highlighted matrine's anti-inflammatory, antioxidant, antimicrobial, and analgesic properties.[13,15] In addition, emerging evidence suggests that matrine effectively reduces TC and TG levels in high diet feed (HFD) mice,[16−19] indicating its potential in HLP treatment. However, the mechanism by which matrine modulates lipid metabolism remains poorly understood, and elucidating this

Received: December 14, 2023
Revised: April 11, 2024
Accepted: April 23, 2024
Published: May 29, 2024

mechanism holds significant potential for advancing its clinical use in HLP treatment.

This study delves into the molecular mechanism underlying the regulation of lipid metabolism disorder by matrine. Through the application of quantitative proteomics, we assessed the dynamic changes in protein expression within HepG2 cells following matrine treatment. Interestingly, we observed a noteworthy increase in LDLR levels. Subsequent validation experiments substantiated that matrine bolsters LDL uptake by modulating LDLR transcription and augmenting protein stability. Furthermore, in vivo experiments showcased matrine's effectiveness in mitigating elevated TC, TG, and LDL-C levels in hyperlipidemic hamsters that had been induced by a high-fat diet. Remarkably, this effect was achieved without influencing body weight or food consumption. Additional investigation unveiled heightened gene transcription and protein expression of LDLR in the livers of matrine-treated hamsters with HLP induced by a high-fat diet. Consequently, LDLR emerges as a pivotal target for matrine's impact on the treatment of HLP.

Similar to the aforementioned phenomenon, we observed that matrine also upregulates the expression of LDLR in A549 cells. A recent study highlighted the potential detrimental effects of excessive low-density lipoprotein (LDL) uptake on breast cancer cells.[20] Therefore, this finding speculates that matrine might exert inhibitory effects on tumor cells by intervening in tumor cell LDL uptake. Furthermore, to identify potential interacting proteins of matrine, we conducted thermal proteome profiling (TPP) analysis, revealing four lipid metabolism-related proteins that could potentially serve as matrine target proteins.

In summary, our quantitative proteomics study has revealed matrine's capacity to upregulate LDLR expression in both HepG2 and A549 cells. Furthermore, we validated that matrine-induced LDLR upregulation significantly contributes to rectifying disordered lipid metabolism in vivo. Our findings thus present a novel avenue for exploring matrine's HLP treatment mechanism and offer a fresh perspective on investigating drug molecular mechanisms.

METHODS

Cell Lines and TMT Agent. The A549 cell line (catalog number: SCSP-503) and HepG2 cell line (catalog number: SCSP-510) were obtained from the National Collection of Authenticated Cell Culture. TMT 10plex was purchased from Thermo Fisher (catalog number: 90111).

Animal Model. We purchased six-week-old healthy male Syrian golden hamsters from Beijing Vital River Laboratory and housed them in the SPF-level Laboratory Animal Room of Shanghai Institute of Materia Medica, Chinese Academy of Sciences. All animal experiments and protocols used in this study were approved by the Animal Ethics Committee of the Shanghai Institute of Materia Medica. This study was conducted under the guidelines and ethics of the Association for Assessment and Accreditation of Laboratory Animal Care International (AAALAC).

We housed hamsters in a light-controlled room at a temperature of 22 °C. The hamsters could access water for free, and they were fed a high-fat diet food (0.5% cholesterol, 23% fat, Research Diets). Before treatment, hamsters were orderly and evenly assigned into the HFD-fed vehicle, HFD-fed matrine-treated, and HFD-fed berberine (BBR)-treated groups according to their serum lipid levels. All of the hamsters were fed a HFD for 4 weeks and orally treated with matrine (50 or 100 mg/kg) or BBR (100 mg/kg) daily for the last 3 weeks. Next, hamsters were euthanized, and their body weights were recorded. The livers of hamsters were immediately removed, cut into small pieces, and saved at −80 °C.

Cell Culture. HepG2 and A549 cells were cultured in Dulbecco's modified Eagle's medium (DMEM, high glucose) supplemented with 10% FBS (164210-50) and 1% P/S (PB180120) in 10 cm dishes (Corning) at 37 °C, 5% CO_2. For proteomics analysis, HepG2 cells were divided into experimental groups and control groups and treated with or without matrine. A549 cells were cultured in DMEM free of lysine/arginine supplemented with 10% dialyzed FBS and either "light" or "heavy" amino acids with 1% penicillin and streptomycin in a 5% CO_2 atmosphere at 37 °C. To ensure that the efficiency of labeling was more than 98%, the cells were cultured for at least 7 generations. A549 cells were treated with matrine or DMSO for 48 h to perform proteomics analysis. For TPP analysis, when A549 cells grew to approximately 80% confluence in the dishes, we divided the cells into experimental groups and control groups and treated them with 1 mM matrine or DMSO for 1.5 h, respectively.

Proteomics Sample Analysis. The treated HepG2 cells and A549 cells were washed with precooled PBS (pepstatin, leupeptin, PMSF) three times. Then, we added RIPA buffer to lyse the cells on ice for 30 min and sonicated them (15 W, 3 min). After centrifugation (16,000*g* at 4 °C for 10 min), we used the BCA assay to determine the protein concentration. For HepG2 cells, 100 μg of proteins were transferred into new tubes. For A549 cells, we equally mixed the proteins from "heavy" and "light" cells and then transferred 100 μg of proteins into new tubes. Next, TCA was used to precipitate the proteins at a final concentration of 10%, and precooled acetone was used to wash the proteins twice. Then, 25 mM Tris buffer (pH 7.5) was used to resuspend the proteins. We added trypsin to the proteins at a ratio of 1:50 overnight to obtain peptide samples. After digestion, the samples were reduced with dithiothreitol (5 mM, 56 °C, 30 min) and alkylated with iodoacetamide (11 mM, room temperature, 30 min).

Thermal Proteome Profiling. The A549 cells were collected after being treated with matrine or DMSO. The collected cells were washed three times and resuspended with precooled PBS. Then, the two groups of cells were equally divided into eight fractions (each of the fractions contained 96 μL of samples), and each fraction was transferred into PCR tubes. The tubes were heated in parallel at different temperatures ranging from 37 to 67 °C at a gradient of 5 °C for 3 min, followed by cooling at 25 °C for 3 min. Subsequently, 10% NP-40 was added to each of the tubes at a final concentration of 4%, and the tubes were incubated on ice for 20 min. After that, the tubes were put into liquid nitrogen to freeze thaw three times. Then, the tubes were subjected to ultracentrifugation at 160,000*g* for 10 min at 4 °C. The supernatant was obtained and moved into fresh tubes. We detected its protein concentration through the BCA assay. Next, we removed 40 μL of the supernatant, reduced it with dithiothreitol (5 mM, 56 °C, 30 min), and alkylated it with iodoacetamide (11 mM, room temperature, 30 min). Finally, the proteins were subjected to short SDS gel electrophoresis.

TMT Labeling. After short SDS gel electrophoresis, we cut the entire lanes of the gel into slices and added ACN to dehydrate them later. After dehydration, the ACN was removed. Trypsin was added to digest the samples in 5 mM

https://doi.org/10.1021/acsomega.3c09983
ACS Omega 2024, 9, 24308−24320

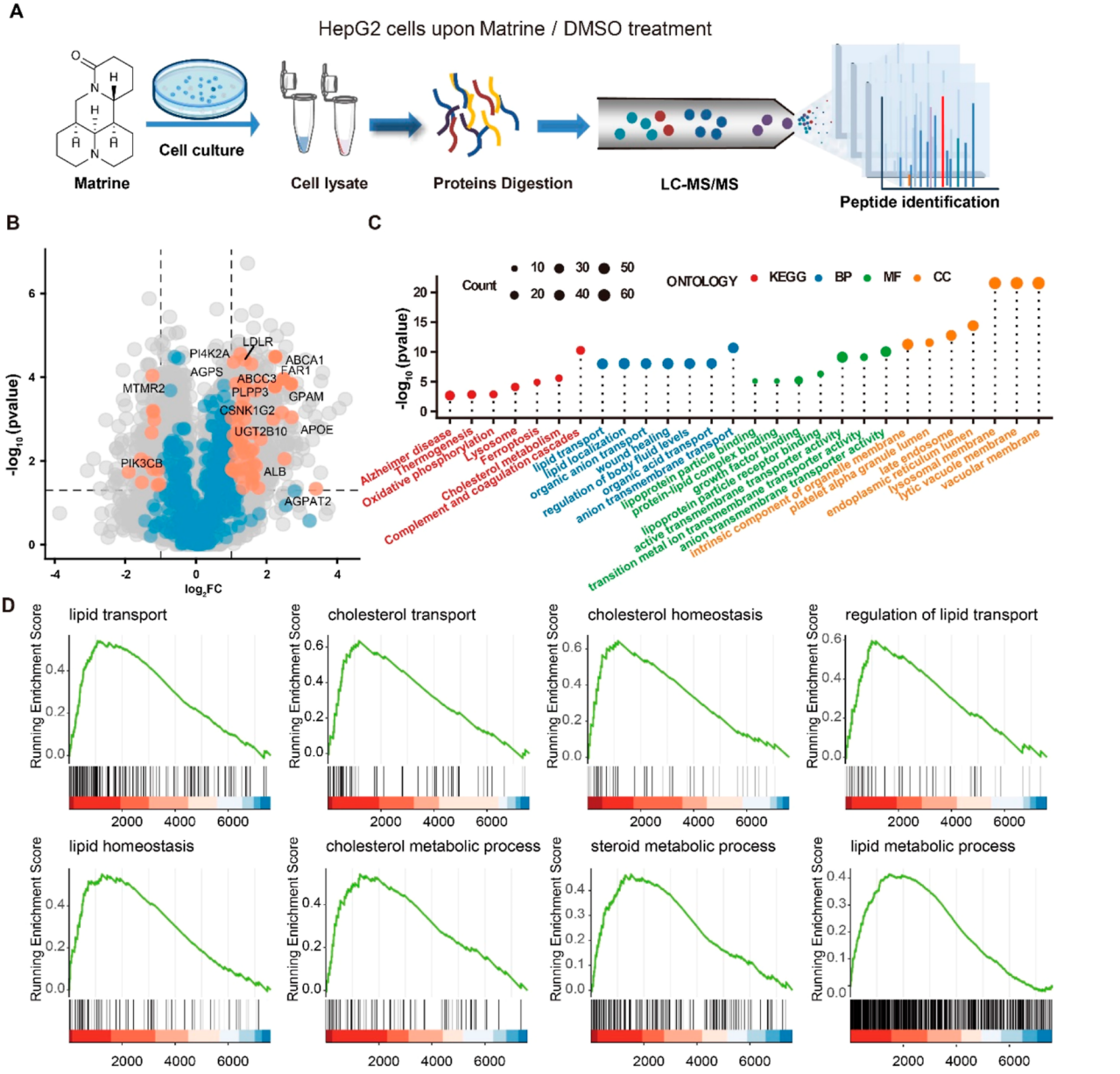

Figure 1. Matrine upregulated proteins enriched in lipid metabolism pathways in HepG2 cells. (A) Chemical structure of matrine and workflow of quantitative proteome analysis. HepG2 cells were treated with or without matrine. Subsequently, proteins were extracted from both groups and subjected to trypsin digestion. The samples were then analyzed using LC−MS/MS. (B) Volcano plot illustrating the dynamic regulation of proteins by matrine. Orange: representative lipid proteins among upregulated proteins; blue: representative lipid proteins among downregulated proteins. (C) KEGG pathway and GO enrichment analysis of upregulated proteins. The top seven enrichment clusters encompassing the KEGG pathway, biological process, cellular component, and molecular function. (D) Gene set enrichment analysis of upregulated proteins.

TEAB buffer (pH 8.0) at 37 °C overnight. Then, we added formic acid until the pH reached 2 to stop the digestion. Next, we added a mixture containing 1% formic acid and 50% ACN to elute and desalt the peptides with a C18-tip after digestion. The desalted peptides were dissolved in 20 μL of 50 mM HEPES at pH 8.5. Subsequently, the TMT (50 μg) solution, which was dissolved in ACN, was added to the peptides and incubated at 25 °C for 1 h. Hydroxylamine was added to stop the reaction at a final concentration of 3% after incubation. Finally, we used a mixture containing 10% FA and 10% ACN to acidize the samples and evaporated them to dryness.

LC−MS/MS Analysis. For TPP analysis, the peptide samples were dissolved in 2 μL of 0.1% FA, and 2 μg of the peptides were loaded on an EASY-nLC 1200 UHPLC system connected to a Q Exactive HF-X mass spectrometer. Then the peptides were injected into a reversed-phase C18 column (20 cm length × 75 μm ID, 1.9 μm particle size, Dr. Maisch GmbH, Germany) in a 60 min gradient from 10 to 90% solvent B (A, 0.1% formic acid; B, 80% acetonitrile in 0.1% formic acid) at 225 nL/min. The eluted peptides were analyzed by the mass spectrometer, which was operated in a data-dependent acquisition mode. During peptide elution, the mass spectrometer method was operated in positive ion mode. Full mass scans were acquired with a mass resolution of 60,000 when the automatic gain control (AGC) number was 3×10^6 and the maximum injection time was 50 ms. The 20 most intensive ions were subjected to fragmentation, with 20 s of dynamical exclusion. The MS2 fragmentation spectra can be

https://doi.org/10.1021/acsomega.3c09983
ACS Omega 2024, 9, 24308−24320

acquired at a resolution of 45,000 when the number of AGC for MS2 is 5×10^4 and the maximum injection time is 65 ms. The fragmentation analysis used HCD with an NCE of 28. The respective data-dependent settings were set with parameters: exclude isotopes as "on"; dynamic exclusion of 60 s using Xcalibur software (available from Thermo Fisher Scientific).

Western Blotting. A549 cells, HepG2 cells, and liver samples were added to RIPA buffer for lysis on ice for 30 min and sonicated at 15 W for 3 min. After centrifugation (16,000*g* at 4 °C for 10 min), we used the BCA assay to determine the protein concentration. Next, proteins were separated by SDS-PAGE electrophoresis and transferred to a PVDF membrane. Then, the membranes were incubated with antibodies against LDLR (Proteintech, Cat# 10785-1-AP, China; 1:2000), PCSK9 (Abcam, Cat# ab181142, UK; 1:2000), and ACTIN (Proteintech, Cat# 66009-1-1g, China; 1:5000). The bands were visualized with an ECL kit and were recorded on a Tanon 4600 (Tanon).

Analysis of Gene Transcription by RT-qPCR. We extracted RNA from cells or liver tissue using TransZol Up regent (TRAN, Cat# ET111, China) and reverse-transcribed RNA to cDNA (Vazyme, Cat# R333-01, China). Real-time PCR was performed on a Steponeplus real-time PCR system with SYBR Green PCR Master mix (Vazyme, Cat# Q712-02, China) and gene-specific primers (LDLR, forward, 5′-CTGAAATCGCCGTGTTACTG-3′, reverse, 5′-GCCAATCCCTTGTGACATCT-3′; PCSK9, forward, 5′-CCAAGCCTCTTCTTACTTCACC-3′, reverse, 5′-GCATCGTTCTGCCATCACT-3′; and Antin, forward, 5′-AGAGCTACGAGCTGCCTGAC-3′, reverse, 5′-AG-CACTGTGTTGGCGTACAG-3′). The relative changes in gene expression were normalized against actin mRNA expression.

DiI-LDL Uptake Analysis. We cultured HepG2 cells in 24-well plates with DMEM supplemented with 1% P/S for 24 h. Then, the cells were incubated in DMEM with 2% LPDS and 20 mg/mL DiI-LDL for 4 h at 37 °C in the dark. After incubation, we used precooled PBS containing 0.4% albumin to wash the cells twice and wash them three times with precooled PBS. Then, we added 400 μL isopropanol into each well and incubated them on a constant shaker at real room temperature for 20 min. Then, 200 μL isopropanol was taken from each well for analysis with a SpectraMax M2e Microplate Reader (Molecular Devices, 520−570 nm).[21]

Serum Lipid Analysis. We collected the blood from hamsters after 16 h of fasting. The serum TC, TG, and LDL-C were enzymatically measured with a kit (Wako, Maccura, Shino, Japan) in an automatic biochemical analyzer (7020, Hitachi, Japan).

Data Analysis. After LC−MS/MS, we used MaxQuant (v1.6.15.0) to retrieve the mass data from the UniProt Human protein database (20376 entries, https://www.uniprot.org). We used TMT 10plex labeling to carry out quantitative analysis. The following settings were used: the maximum missed cleavage sites were 2, carbamidomethylation of cysteine was set as the fixed modification, and the oxidation of methionine and N-terminal acetylation were specified as variable modifications. We set the lowest temperature point at 1 and calculated the comparison between the relative abundances of the TMT reporter ions with the lowest temperature to determine melting points. Then, we used the TPP R script to normalize the data, and the following equation was used to fit the melting curve of proteins. When half of the protein is denatured at this temperature, the melting point of the protein is $f(T) = 0.5$.

$$f(T) = \frac{1 - \text{plateau}}{1 + e^{-\left(\frac{a}{T} - b\right)}} + \text{plateau}$$

Bioinformatic Analysis. For the cellar pathway analysis, GO analysis, KEGG pathway analysis, and GSEA were performed for a hypergeometric test in the clusterProfiler package in R. The ClueGO app was used to find over-represented KEGG pathway and Reactome pathway and a network of connected those terms was created. The proteins identified as having matrine-dependent thermostability were put into the STRING database (v11, http://www.string-db.org/) to build the protein−protein association network and visualized in Cytoscape (v.3.8.2). Finally, StringAPP embedded in Cytoscape (v1.7.0) was used to enrich the key network of protein−protein interactions (PPIs) by function.[22]

RESULTS

Quantitative Proteomics Analysis of HepG2 Cells upon Matrine Treatment. Matrine is a natural alkaloid with pharmacological activity in the treatment of HLP (Figure 1A). In order to delve into the mechanism through which matrine regulates disrupted lipid metabolism, we examined its impact on the HepG2 proteome by treating cells with or without matrine. The IC_{50} of matrine on HepG2 cells was determined to be 5.066 mM following a 48 h treatment, exhibiting minimal impact on HepG2 cell proliferation when the dose was below 1.25 mM. Following treatment, we extracted proteins from both groups, which were subsequently subjected to trypsin digestion and prepared for LC−MS/MS analysis. Data analysis was performed using MaxQuant software (Figure 1A).

The quantitative proteome analysis through LC−MS/MS yielded the quantification of a total of 7582 proteins (Figure 1B, Supporting Information Table S1). Out of these, 854 proteins displayed distinct expression patterns when compared with the control group ($|\log_2$ (Fold change)$| > 1$, P value <0.05). Notably, 600 proteins exhibited upregulation upon matrine treatment ($\log_2$ (Fold change) > 1, P value <0.05), whereas 253 proteins showed downregulation ($\log_2$ (Fold change) < −1, P value <0.05). Importantly, a significant portion of these dynamically altered proteins showed correlations with lipid metabolism, exemplified by LDLR ($\log_2$ (Fold change) = 1.379).

Pathways and Biological Process in HepG2 Cells Affected by Matrine Treatment. To elucidate the potential cellular pathways influenced by the upregulated proteins induced by matrine, we performed enrichment analysis using the KEGG database (Figure 1C). Interestingly, the upregulated proteins exhibited enrichment in cholesterol metabolism (adjusted $p = 3.08 \times 10^{-6}$ -), lysosome (adjusted $p = 9.01 \times 10^{-5}$), and thermogenesis (adjusted $p = 1.75 \times 10^{-3}$). These enrichment results suggest a robust impact of matrine on lipid metabolism, particularly cholesterol metabolism.

To further explore the influence of matrine on cellular process, we performed enrichment analysis using the Gene Ontology (GO) database (Figure 1C). The top seven enriched biological process clusters primarily revolved around material transport, encompassing lipid transport (adjusted $p = 1.3 \times 10^{-8}$) and lipid localization (adjusted $p = 1.1 \times 10^{-8}$). This result underscores matrine's influence on lipid transport,

https://doi.org/10.1021/acsomega.3c09983
ACS Omega 2024, 9, 24308−24320

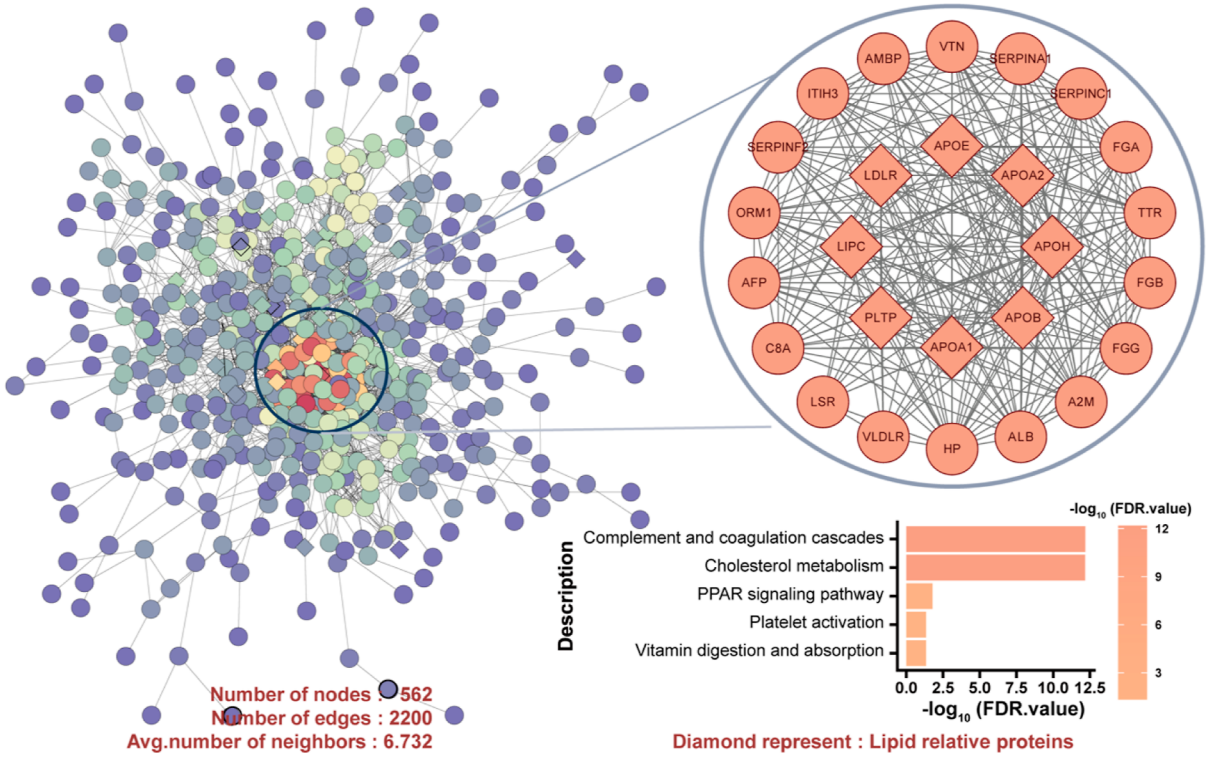

Figure 2. PPI analysis of upregulated proteins mediated by matrine in HepG2 cells. The graph depicts PPIs, with each pattern representing a protein. Diamonds symbolize proteins associated with lipid metabolism, and darker areas indicate closer connections.

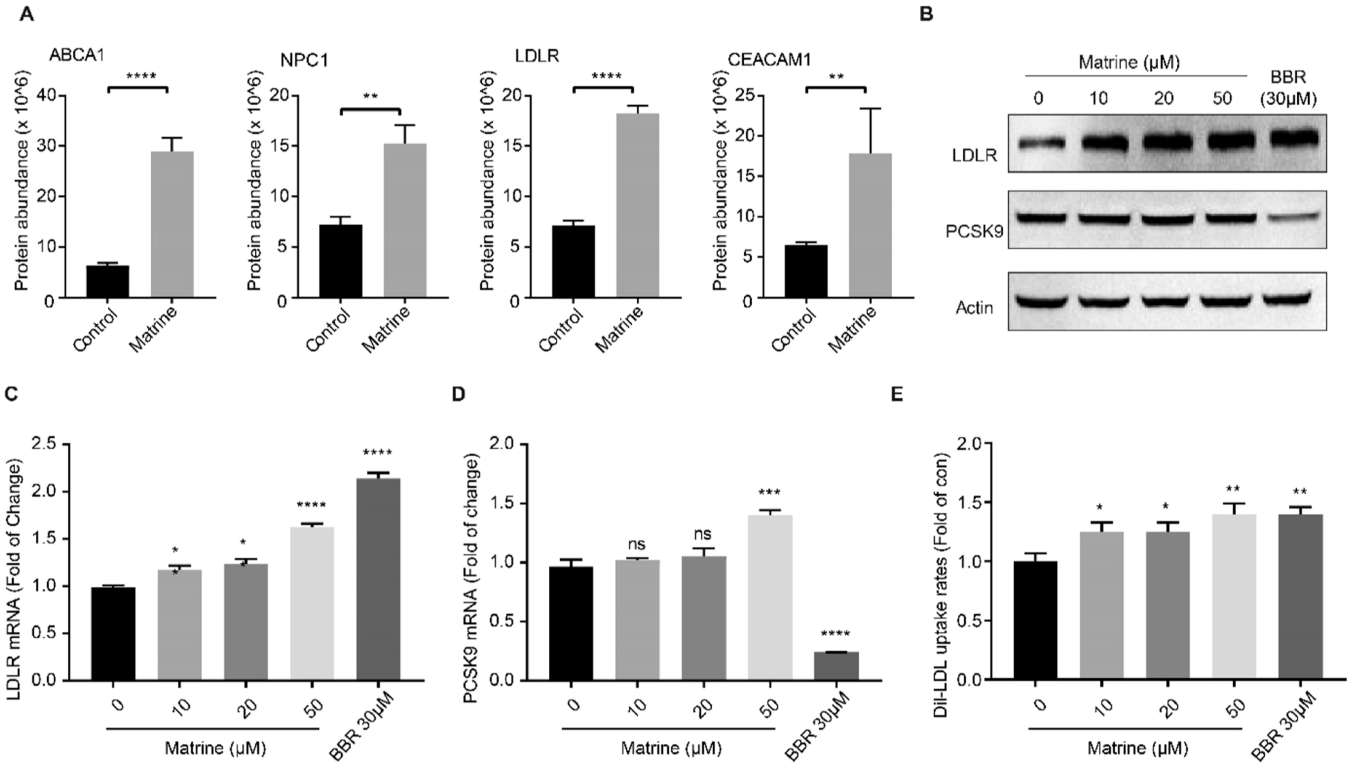

Figure 3. Matrine upregulated gene transcription and expression of LDLR in HepG2 cells. (A) Candidate proteins related to lipid metabolism. (B) Western blot validation of matrine-induced dose-dependent upregulation of LDLR protein expression in HepG2 cells, while having little effect on PCSK9 protein. (C) RT-qPCR validation of matrine-induced dose-dependent upregulation of LDLR gene transcription in HepG2 cells. (D) RT-qPCR validation indicating that matrine had little effect on PCSK9 gene transcription in HepG2 cells. (E) Dil-LDL uptake analysis revealing that matrine promoted the uptake of LDL by HepG2 cells.

https://doi.org/10.1021/acsomega.3c09983
ACS Omega 2024, 9, 24308−24320

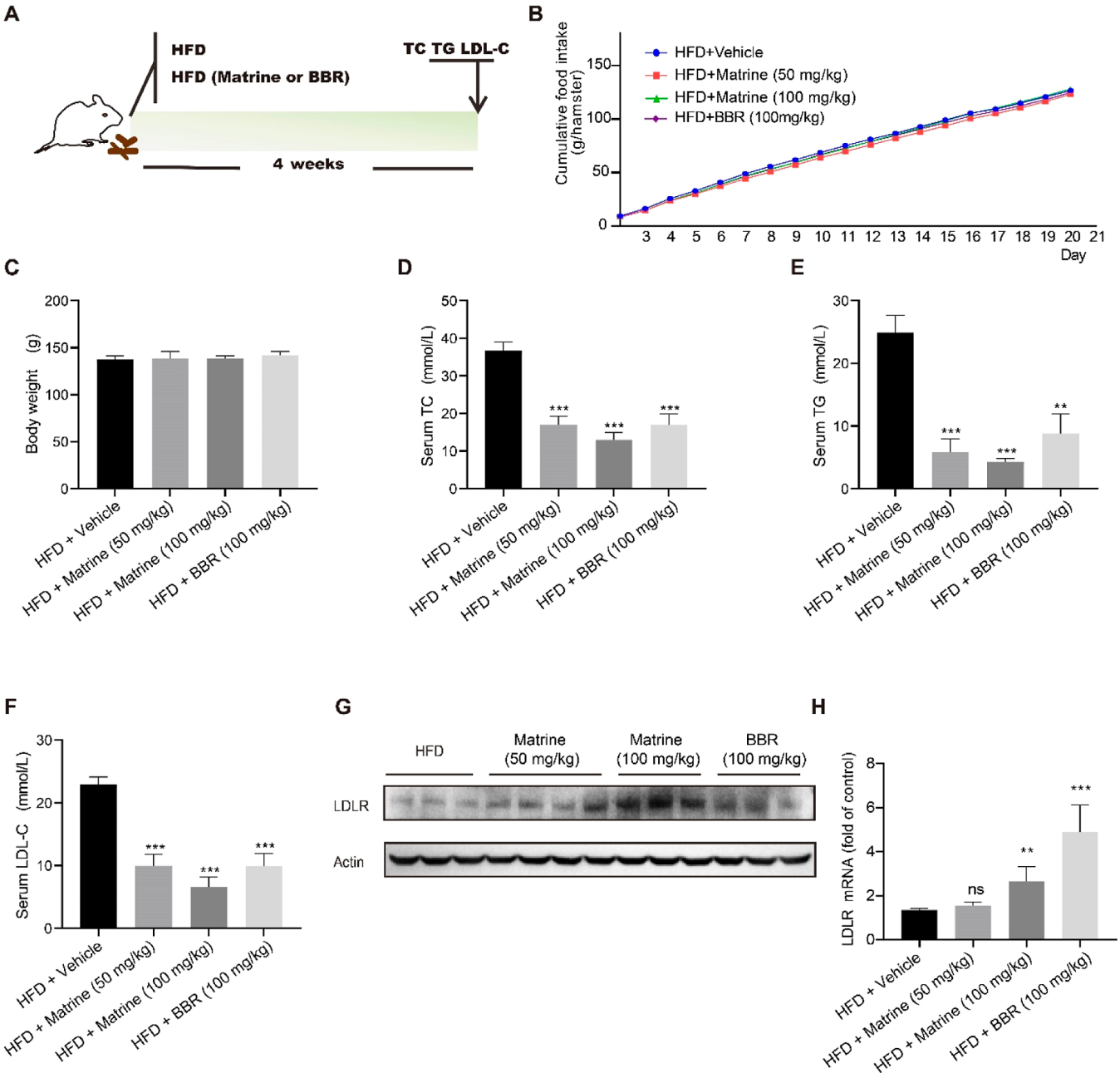

Figure 4. Matrine reversed disordered lipid metabolism in HFD hamsters. (A) Experimental procedure for the animal study. Hamsters were subjected to a high-fat diet (HFD) for 4 weeks and subsequently treated with matrine (50 or 100 mg/kg) or BBR (100 mg/kg) during the last 3 weeks. Serum lipids analysis was conducted on the last day. (B) Graph illustrating the cumulative food intake of hamsters. (C) Body weight of hamsters in the last day. (D) Alterations in TC levels in response to matrine administration in hamsters. (E) Alterations in TG levels in response to matrine administration in hamsters. (F) Alterations in LDL-C levels in response to matrine administration in hamsters. (G) Western blot validation of matrine-induced upregulation of LDLR protein expression in hamster livers. (H) RT-qPCR validation of matrine-induced upregulation of LDLR gene transcription in hamster livers.

aligning with the KEGG database results. Additionally, the top seven enriched cellular component clusters revealed that the upregulated proteins mainly constituted the cell membrane components, such as the lysosomal membrane (adjusted $p = 4.1 \times 10^{-21}$). Similarly, the enriched clusters of molecular function highlighted that the upregulated proteins predominantly engaged in transmembrane transporter activity, such as anion transmembrane transporter activity (adjusted $p = 1.2 \times 10^{-10}$) and active transmembrane transporter activity (adjusted $p = 1.0 \times 10^{-9}$). The molecular function enrichment implies that matrine enhances cellular metabolism. Together, these results suggested that matrine-induced upregulated proteins primarily reside within the cell membrane, exhibit transmembrane transporter functions, and are related to lipid transport.

Next, we performed Gene Set Enrichment Analysis (GSEA) with the GO database (Figure 1D). The upregulated proteins significantly enriched processes such as lipid transport (adjusted $p = 2 \times 10^{-2}$), cholesterol transport (adjusted $p = 2 \times 10^{-2}$), cholesterol homeostasis (adjusted $p = 2 \times 10^{-2}$), regulation of lipid transport (adjusted $p = 2 \times 10^{-2}$), lipid homeostasis (adjusted $p = 2 \times 10^{-2}$), cholesterol metabolic

https://doi.org/10.1021/acsomega.3c09983
ACS Omega 2024, 9, 24308−24320

process (adjusted $p = 2 \times 10^{-2}$), steroid metabolic process, and lipid metabolic process (adjusted $p = 2 \times 10^{-2}$). This outcome further substantiates matrine's role in enhancing lipid metabolism, cholesterol metabolism, and sterol metabolism. Together with the above results, matrine may execute its disordered lipid metabolism regulatory function by bolstering cellular lipid metabolism and lipid transport.

To further elucidate the mechanism under lipid metabolism regulation of matrine, we conducted PPI analysis among the upregulated proteins using the STRING database and employed StringAPP, which facilitates the integration of STRING networks into Cytoscape[22] (Figure 2). In the interaction network, darker connections signify closer associations. The upregulated proteins demonstrated enrichment in cholesterol metabolism, vitamin digestion, and vitamin absorption. The transport of cholesterol and the metabolism of vitamins are pertinent to lipid metabolism.[23,24] In addition, proteins presented as diamonds are linked to lipid metabolism. This observation offers further evidence that matrine indeed stimulates lipid metabolism.

LDLR Is Upregulated in HepG2 Cells upon Matrine Treatment. Subsequently, our investigation into matrine's potential as a therapeutic intervention for HLP directed our attention toward the identification of specific proteins associated with lipid metabolism within the cohort of the upregulated proteins (Figure 3A).

ATP-binding cassette transporter A1 (ABCA1) ($\log_2$(Fold change) = 2.247) emerges as a crucial member of the ABCA subfamily of ATP-binding cassette transporters, pivotal in facilitating the loading of apoA-1 with phospholipids to form high-density lipoproteins (HDLs).[25] Notably, mutations in ABCA1 have been implicated in Tangier disease, an uncommon and severe form of HDL deficiency characterized by an impairment in cellular cholesterol efflux.[26,27] Thus, it is conceivable that matrine may elevate ABCA1 expression, thereby fostering HDL formation and potentially ameliorating disordered lipid metabolism.

Carcinoembryonic antigen-related cell adhesion molecule 1 (CEACAM1) ($\log_2$(Fold change) = 1.396), a transmembrane glycoprotein primarily found in the liver,[28] has been associated with insulin resistance, fatty liver disease, and obesity when subjected to mutations. CEACAM1 overexpression has been demonstrated to possess the ability to counteract hyperinsulinemia, notably reducing insulin resistance and hepatic lipid accumulation.[29,30] Hypothetically, matrine's efficacy in treating HLP might be attributed to its upregulation of CEACAM1 expression.

The involvement of NPC intracellular cholesterol transporter 1 (NPC1) ($\log_2$(Fold change) = 1.188), a transmembrane glycoprotein pivotal in transferring LDL-C from late endosome or lysosome to the endoplasmic reticulum for esterification or the plasma membrane for efflux,[31] presents another avenue. Studies have shown that NPC1 upregulation enhances cholesterol transport and inhibits foam cell formation.[31,32] Hence, matrine-induced upregulation of NPC1 might contribute to the regulation of lipid metabolism.

Remarkably, LDLR ($\log_2$(Fold change) = 1.378), a cell surface glycoprotein that plays a pivotal role in maintaining plasma cholesterol levels through endocytosis of LDL-C,[33] could potentially benefit from matrine-induced upregulation, facilitating increased extracellular uptake of LDL-C and aligning with its role in treating HLP.

Intriguingly, our investigation demonstrated matrine's dose-dependent upregulation of LDLR (Figure 3B). Moreover, we evaluated the influence of matrine on Pro-protein convertase subtilisin-like/kexin type 9 (PCSK9), a factor involved in mediating LDLR degradation.[34] We employed BBR as a positive control, a compound known to downregulate PCSK9 and consequently enhance LDLR expression. Encouragingly, our results indicated the minimal influence of matrine on PCSK9. The upregulation of LDLR protein level typically results from either PCSK9-mediated mechanisms or the promotion of LDLR gene transcription. Therefore, to ascertain that matrine-mediated LDLR upregulation occurs through gene transcription promotion, we performed RT-qPCR analysis. Our findings aligned with protein expression data, revealing that matrine indeed upregulated LDLR mRNA levels in a dose-dependent manner. Notably, matrine exerted little influence on PCSK9 mRNA levels (Figure 3C,D).

Moreover, the primary function of LDLR is the uptake of LDL-C from extracellular environments.[35] To evaluate matrine's impact on the function of LDLR, we cultured HepG2 cells and treated cells with matrine under starving conditions and subsequently exposed cells to fluorescently labeled Dil-LDL. Our fluorescence-based assessment of cellular LDL uptake mirrored the protein expression outcomes, underscoring matrine's capacity to promote LDL uptake in a dose-dependent manner (Figure 3E).

Disordered Lipid Metabolism Is Reversed by Matrine in Hyperlipidemic Hamsters. In order to validate the lipid-lowering efficacy of matrine in vivo, we established a hyperlipidemic hamster model by administering a HFD (Figure 4A). The hamsters subjected to the HFD regimen were subsequently treated with either a vehicle (0.5% CMC-Na) or matrine (at doses of 50 or 100 mg/kg) for a duration of 21 days. The positive control group received treatment with BBR at a dose of 100 mg/kg. Following the treatment period, we assessed the level of TC, TG, and LDL-C in the hamster blood.

Our observations indicated that the cumulative food intake and the body weight of the hamster remained unaffected by the administration of matrine or BBR (Figure 4B,C). However, there was a noteworthy reduction in the levels of TC, TG, and LDL-C after the matrine or BBR treatments (Figure 4D−F). Interestingly, matrine exhibited a superior regulatory effect on serum TC, TG, and LDL-C levels in comparison to BBR, particularly at the higher dosage (100 mg/kg).

To investigate whether matrine's impact on LDLR levels in vivo mirrored its effect in cells, we assessed the hepatic LDLR expression in hamsters (Figure 4G). As anticipated, both matrine and BBR treatment led to an upregulation in the expression of LDLR. Remarkably, the high-dosage matrine group (100 mg/kg) displayed a more pronounced increase in LDLR expression compared to the low-dosage group (50 mg/kg). Similarly, at the same dose, matrine (100 mg/kg) exhibited a more potent upregulation of LDLR compared to BBR (100 mg/kg). Furthermore, we analyzed the mRNA levels of LDLR (Figure 4H). These results clearly demonstrated an upregulation of LDLR levels following matrine or BBR treatment. Interestingly, BBR exhibited elevated levels of LDLR mRNA expression; however, this did not correspond with protein expression levels under high-dose matrine treatment. Emerging studies have suggested that numerous processes influence the relationship between protein and mRNA abundance, including translational regulation, modu-

https://doi.org/10.1021/acsomega.3c09983
ACS Omega 2024, 9, 24308−24320

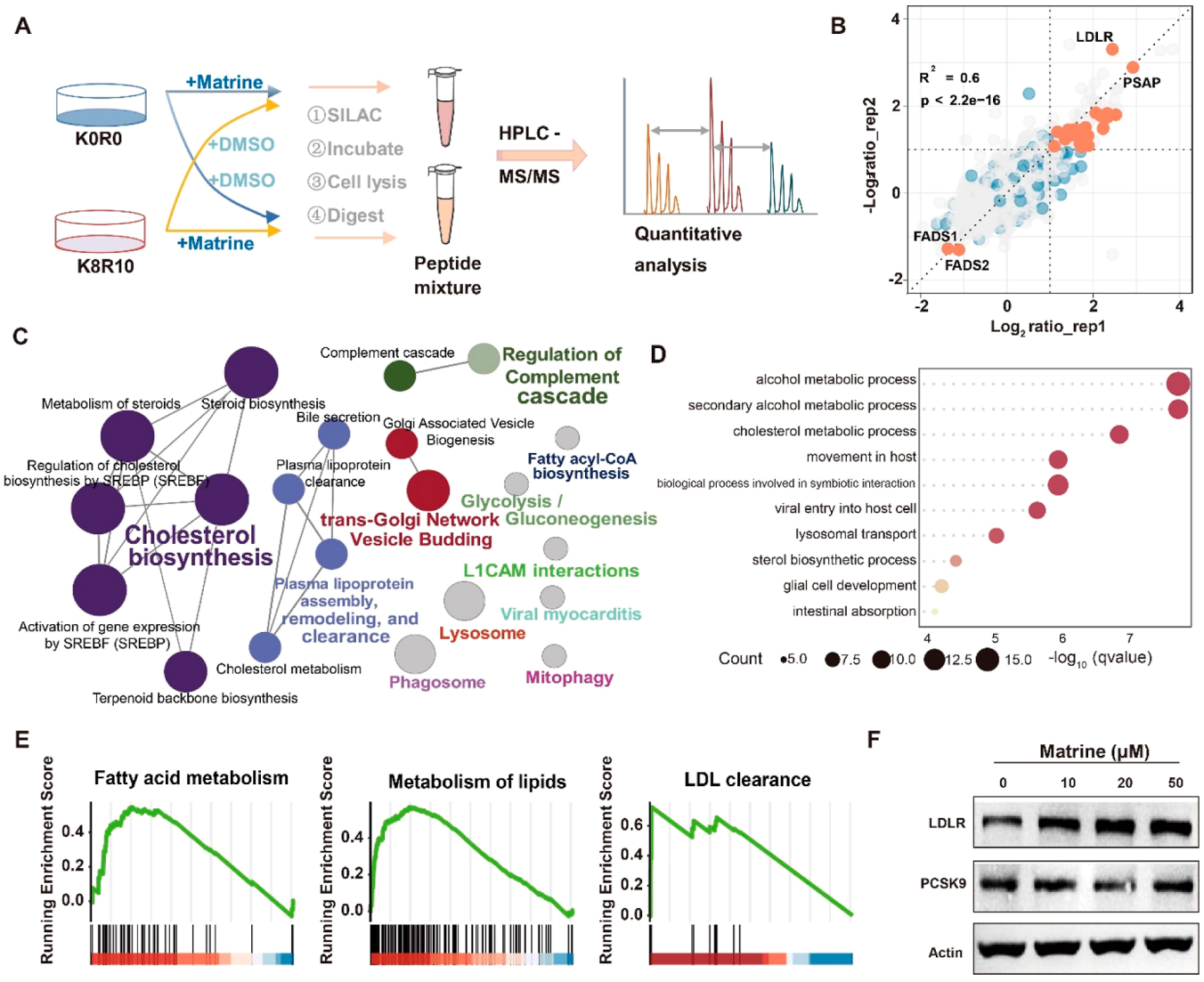

Figure 5. Matrine-induced upregulated proteins enriched in pathways associated with lipid metabolism in A549 cells. (A) Workflow of quantitative proteome analysis. A549 cells were cultured in a medium with either "light" or "heavy" amino acids and treated with or without matrine. After treatment, proteins from both groups were equally combined after extraction and subjected to trypsin digestion. The samples were subsequently analyzed by LC−MS/MS. (B) Graph illustrating quantified proteins in two replicates. Orange: dynamic lipid proteins; blue: stable lipid proteins. (C) KEGG and Reactome pathway analysis of upregulated proteins. Each node represents a term, and the colors represent the pathway group. The edges reflect the relationships between the terms based on the similarity of their associated genes. (D) GO enrichment analysis of upregulated proteins. The top ten enrichment clusters of biological processes are presented. (E) Gene Set Enrichment Analysis of upregulated proteins. (F) Western blot validation of matrine-induced dose-dependent upregulation of LDLR protein expression in A549 cells, with little effect on PCSK9 protein.

lation of protein stability, protein synthesis delay, and others.[36] Consequently, the induction of LDLR protein expression by BBR may also be subject to these processes, resulting in a lack of high consistency between its abundance and mRNA levels. Collectively, these results suggested that matrine can attenuate serum TC, TG, and LDL-C levels by stimulating gene transcription and protein expression of LDLR in vivo.

Although studies have reported potential liver toxicity from administering matrine at doses of 118 and 154 mg/kg/day for 21 days in mice,[13] our study did not observe matrine-induced liver toxicity, even at a high dose (100 mg/kg/day).

Influence of Matrine on the Proteome of A549 Cells. A growing body of evidence has demonstrated that matrine possesses therapeutic potential for various cancers, including lung cancer.[37,38] Given that disordered lipid metabolism has been identified as a crucial factor in the progression of lung cancer,[39] we hypothesize that matrine's antitumor effects might stem from its regulation of lipid metabolism.

To elucidate the mechanism underlying matrine's efficacy against lung cancer, we conducted a comprehensive investigation of its impact on the proteome of A549 cells. In this strategy, we employed stable isotope labeling of amino acids in cell cultures (SILAC). After the treatment with matrine ("light" labeling) or DMSO ("heavy" labeling), we extracted proteins from both groups and combined them at a 1:1 ratio. In a biological replicate experiment, the SILAC labeling is reversed. These samples were then subjected to trypsin digestion and prepared for LC−MS/MS analysis, with data analysis executed using the MaxQuant software (Figure 5A). To enhance the robustness of our findings, we performed label-swapping repetitions.

https://doi.org/10.1021/acsomega.3c09983
ACS Omega 2024, 9, 24308−24320

Through the quantitative proteome analysis, we successfully quantified a total of 2533 proteins (Figure 5B, Supporting Information Table S2). Among these, 76 proteins were upregulated ($\log_2$ (Fold change) > 1, P value <0.05) while 7 proteins were downregulated ($\log_2$ (Fold change) < −1, P value <0.05). Particularly noteworthy was the remarkable upregulation of LDLR among the elevated proteins in response to matrine treatment. Intriguingly, a separate study has proposed that increased LDL can foster tumor growth, yet enhanced and prolonged LDL uptake is associated with heightened caspase-3 cleavage, a detrimental process for breast cancer cells.[20]

As a consequence, we postulate that matrine's antilung cancer effects might stem from its ability to elevate LDLR expression and sustain LDL uptake, thereby potentially impeding lung cancer progression. This insight underscores the intricate interplay between matrine, lipid metabolism, and cancer modulation.

Pathways and Biological Process in A549 Cells Affected by Matrine Treatment. To elucidate the potential pathway modulated by matrine in A549 cells, we performed KEGG and Reactome pathway enrichment analysis using upregulated proteins induced by matrine treatment (Figure 5C). Our observations revealed significant enrichment of upregulated proteins within pathways related to cholesterol biosynthesis, plasma lipoprotein assembly, remodeling, and clearance, and fatty acyl-CoA biosynthesis. This result underscores the substantial impact of matrine on cell metabolism. Notably, the upregulation of the steroid biosynthesis (adjusted $p = 1.299 \times 10^{-3}$) and cholesterol metabolism (adjusted $p = 9.38 \times 10^{-2}$) pathways implies that matrine continues to influence lipid-related metabolic pathways within A549 cells.

Moreover, we performed enrichment analysis with the GO database to probe the effects of matrine on the cellular process (Figure 5D). The most prominent biological process clusters include the alcohol metabolic process (adjusted $p = 2.128 \times 10^{-8}$), secondary alcohol metabolic process (adjusted $p = 2.128 \times 10^{-8}$), and cholesterol metabolic process (adjusted $p = 1.586 \times 10^{-7}$). The results of the biological process enrichment analysis parallel those obtained from the KEGG database, signifying the profound influence of matrine on lipid metabolism in A549 cells.

Additionally, we performed GSEA utilizing the Reactome database (Figure 5E). As expected, the upregulated proteins exhibited pronounced enrichment in fatty acid metabolism (adjusted $p = 2.18 \times 10^{-2}$), metabolism of lipids (adjusted $p = 2.18 \times 10^{-2}$), and LDL clearance (adjusted $p = 2.99 \times 10^{-2}$). To delve further, we explored the interplay among differentially expressed proteins through the STRING database (Supporting Information Figure S1). Consistent with the above results, the upregulated proteins exhibited strong correlations with lipid metabolism.

Together, matrine unquestionably wields a potent influence on lipid metabolism pathways. Furthermore, we corroborated the enhancement of LDLR expression by matrine (Figure 5F). Nevertheless, whether matrine exerts its antilung cancer function through LDLR upregulation, subsequently prolonging LDL uptake, necessitates further in-depth investigation.

Identification of Potential Protein Targets of Matrine through TPP. In pursuit of potential protein targets of matrine, we performed TPP analysis. TPP is a method that integrates the Cellular Thermal Shift Assay (CETSA) with quantitative mass spectrometry. This approach is based on the concept of ligand-induced thermostabilization of target proteins, providing insights into the affinity between drugs and target proteins derived from cellular or tissue samples.[40−42]

Considering the practical research requirements, we conducted the TPP experiments only on A549 cells. Initially, A549 cells were treated with matrine or DMSO for 1.5 h. Subsequently, cells from both groups were harvested and divided into eight aliquots for gradual heating. After heating, the samples underwent lysis using 1% NP-40, and the supernatant containing soluble proteins was collected through centrifugation. Although pellet analysis is considered helpful in identifying more binding proteins in a small number of studies,[43] the most widely accepted TPP method currently involves analyzing the supernatant after heating. Therefore, we employed the well-established method. The soluble proteins were then labeled using Tandem Mass Tag (TMT) reagent and subjected to LC−MS/MS analysis (Supporting Information Figure S2A). To ensure the robustness of our experiment, we conducted two replications, and a high degree of correlation was evident between these replications (Supporting Information Figure S2B).

Data analysis of the TPP revealed a total of 5398 identified proteins (Supporting Information Table S3). Within these, 4322 proteins were identified in the matrine-treated group, while 4319 proteins were identified in the DMSO-treated group. Given the denaturation and insolubilization of proteins upon exposure to heat,[44] a reduction in the abundance of soluble proteins was indeed observed with increasing temperature (Supporting Information Figure S2C).

Next, we selected 3729 proteins that were identified in both matrine-treated and DMSO-treated groups to generate melting curves. Unfortunately, 1206 proteins were unable to generate a melting curve due to the presence of some missing values. We subsequently compared the melting points of the remaining 2523 proteins. The results indicated an increase in the melting point for some proteins in the matrine-treated group compared to the same proteins in the DMSO-treated group (Supporting Information Figure S2D). These proteins were ranked based on the magnitude of their ΔTm ($\Delta Tm = |Tm(\text{matrine}) - Tm(\text{DMSO})|$) (Supporting Information Figure S2E). Of note, 115 proteins were shown as orange data points with $\Delta Tm > 1$ and a p value <0.05, signifying a significant thermal shift (Supporting Information Figure S2F). To reinforce the reliability of the experiment, proteins were required to be identified in both biological replicates (Supporting Information Figure S2G). Ultimately, we pinpointed 76 candidate proteins.

Among these candidate proteins, we identified four linked to lipid metabolism (Supporting Information Table S4 and Figure S3). Notably, voltage-dependent anion-selective channel protein 1 (VDAC1) is a mitochondrial porin involved in apoptosis and influenced by lipids.[45] Delta (24)-sterol reductase (DHCR24) is a critical enzyme in cholesterol biosynthesis.[46,47] Acyl-coenzyme A diphosphatase FITM2 (FITM2) is an endoplasmic membrane protein implicated in promoting lipid accumulated in cell culture.[47] In addition, ABCD3 is an ATP-dependent transporter within the ATP-binding cassette (ABC), playing a pivotal role in fatty acids or fatty acyl-coenzyme A transport.[48] Moreover, we performed enrichment analysis with the GO database to probe the effects of the other 72 proteins (Supporting Information Figure S4). Interestingly, the most prominent biological process clusters of

https://doi.org/10.1021/acsomega.3c09983
ACS Omega 2024, 9, 24308−24320

these proteins were mainly involved in the cellular nitrogen compound metabolic process (adjusted $p = 4.90 \times 10^{-3}$) and nitrogen compound metabolic process (adjusted $p = 6.20 \times 10^{-3}$). These pathways are closely related to lipid metabolism, as lipid synthesis is influenced by the glutamate dehydrogenase pathway, and the main product of this pathway, glutamine, plays a crucial role in nitrogen metabolism.[49,50] This result suggests a potential association between matrine and lipid metabolism, with these four proteins serving as potential targets of matrine in cancer therapy.

DISCUSSION

This study delves into the molecular mechanism underlying Matrine's potential for HLP treatment using quantitative proteomics. In HepG2 cells, we observed that matrine upregulated both the mRNA and protein levels of LDLR, subsequently enhancing Dil-LDL uptake by the cells. Remarkably, this effect extended to the livers of hamsters, with matrine similarly upregulating LDLR expression. Additionally, we demonstrated that matrine effectively ameliorated disordered lipid metabolism in hamsters fed with HFD. Both in vitro and in vivo experiments firmly established that matrine's HLP-treating prowess involves the upregulation of LDLR expression. Based on the results from our study and literature, we speculate that matrine may potentially impact LDLR mRNA expression through various mechanisms, such as by influencing the activity of transcription factors to regulate LDLR gene transcription, or by affecting the stability of LDLR mRNA to regulate its levels. However, our current data are not sufficient to derive the exact mechanism. To explore potential protein targets of matrine, we attempted TPP experiments and observed significant effects of matrine on several lipid metabolism proteins. Further analysis revealed that matrine can also influence the lipid biosynthetic process and nitrogen metabolic pathway. Based on these findings, we hypothesize that matrine not only alters LDLR expression levels through transcriptional regulation but also modulates lipid metabolism by affecting metabolic pathway proteins. In addition, since matrine primarily influences lipid metabolism and other metabolic pathways, metabolomics research will undoubtedly enhance our understanding of matrine's metabolic regulation in future studies,[51,52] which will provide a more comprehensive insight into the molecular pathways modulated by matrine.

Recognizing the connection between disrupted metabolism and cancer development, and taking into account the documented potential of matrine for antilung cancer activity, we also sought to determine whether matrine's anticancer effect is mediated by its regulation of disordered lipid metabolism. Astonishingly, our investigation revealed that matrine-induced upregulated proteins in A549 cells were predominantly enriched in lipid metabolism-related pathways. More intriguingly, matrine also upregulated LDLR expression in A549 cells. Given that increased LDLR expression and extended LDL uptake can prove detrimental to cancer cells, our primary results have provided valuable insights into the anticancer properties of matrine.

Currently, statins remain the primary choice for HLP treatment.[7] Statins, acting as inhibitors of HMG-CoA reductase, curb cholesterol biosynthesis, induce LDLR upregulation through feedback, and subsequently bolster LDL uptake. However, about 15% of patients fail to achieve target HLP treatment goals with statins alone.[53,54] Therefore, alternative nonstatin medications have been explored. For example, PCSK9 inhibitors, including monoclonal antibodies and small molecules, have emerged as clinical options.[55,56] Given the differing mechanisms of action among matrine, PCSK9 inhibitors, and statins, their combined usage holds the potential to yield favorable therapeutic effects.

TPP is currently one of the most powerful tools for investigating drug−protein interactions, yet it also has the potential to result in the loss of such interaction information. For instance, certain proteins may degrade at extremely high or low temperatures, or some may show insignificant changes in thermal stability following matrine binding. Moreover, mass spectrometry-based proteomics techniques may not comprehensively reflect all proteins in the sample, particularly those with lower abundance yet crucial in the system. In our study, TPP analysis identified 76 potential matrine-binding proteins, primarily concentrated in metabolic pathways. Despite matrine exhibiting potent pharmacological activity, its binding proteins largely remain unidentified, thereby rendering our findings valuable in providing data support for matrine target discovery. Further biological experiments are also necessary to confirm the existence of these targets.

CONCLUSIONS

This study investigated the molecular mechanism underlying matrine's potential for treating HLP in in vitro and in vivo experiments. Employing quantitative proteomics, we discovered that matrine increases the expression of LDLR in cells, with subsequent experiments validating its role in enhancing LDL uptake. It effectively lowers lipid levels in hyperlipidemic hamsters without affecting body weight, indicating LDLR as a critical target for matrine's impact on HLP.

ASSOCIATED CONTENT

Data Availability Statement

The mass spectrometry proteomics data have been deposited to the ProteomeXchange Consortium via the PRIDE partner repository with the data set identifier PXD045502.

Supporting Information

The Supporting Information is available free of charge at https://pubs.acs.org/doi/10.1021/acsomega.3c09983.

Protein−protein interaction (PPI) analysis of upregulated proteins mediated by matrine in A549 cells; identification of potential protein targets of matrine through TPP; thermal melt curves of representative proteins VDAC1, DHCR24, FITM2, and ABCD3; GO enrichment analysis of 72 proteins (PDF)

Proteomic data from HepG2 cells treated with matrine/DMSO (XLSX)

SILAC labels proteomic data from A549 cells upon matrine/DMSO treatment (XLSX)

Thermal proteome profiling results (XLSX)

Thermal melt points of representative proteins VDAC1, DHCR24, FITM2, and ABCD3 (XLSX)

AUTHOR INFORMATION

Corresponding Author

He Huang − *School of Chinese Materia Medica, Nanjing University of Chinese Medicine, Nanjing 210203, China; State Key Laboratory of Chemical Biology, Shanghai Institute of Materia Medica, Chinese Academy of Sciences, Shanghai 201203, China; School of Pharmaceutical Science and Technology, Hangzhou Institute for Advanced Study,*

https://doi.org/10.1021/acsomega.3c09983
ACS Omega 2024, 9, 24308−24320

University of Chinese Academy of Sciences, Hangzhou 310024, China; Shandong Laboratory of Yantai Drug Discovery, Bohai Rim Advanced Research Institute for Drug Discovery, Yantai 264117, China; orcid.org/0000-0001-6998-8131; Email: hhuang@simm.ac.cn

Authors

Huixu Feng − *School of Chinese Materia Medica, Nanjing University of Chinese Medicine, Nanjing 210203, China; State Key Laboratory of Chemical Biology, Shanghai Institute of Materia Medica, Chinese Academy of Sciences, Shanghai 201203, China*

Guobin Liu − *School of Chinese Materia Medica, Nanjing University of Chinese Medicine, Nanjing 210203, China; State Key Laboratory of Chemical Biology, Shanghai Institute of Materia Medica, Chinese Academy of Sciences, Shanghai 201203, China*

Luhan Li − *School of Life Science and Technology, ShanghaiTech University, Shanghai 201210, China; State Key Laboratory of Drug Research, Shanghai Institute of Materia Medica, Chinese Academy of Sciences, Shanghai 201203, China*

Xuelian Ren − *State Key Laboratory of Chemical Biology, Shanghai Institute of Materia Medica, Chinese Academy of Sciences, Shanghai 201203, China*

Yue Jiang − *State Key Laboratory of Chemical Biology, Shanghai Institute of Materia Medica, Chinese Academy of Sciences, Shanghai 201203, China; School of Mechanical Engineering and Automation, Northeastern University, Shenyang 110819, China*

Wanting Hou − *State Key Laboratory of Chemical Biology, Shanghai Institute of Materia Medica, Chinese Academy of Sciences, Shanghai 201203, China*

Ruilong Liu − *State Key Laboratory of Chemical Biology, Shanghai Institute of Materia Medica, Chinese Academy of Sciences, Shanghai 201203, China*

Kun Liu − *School of Mechanical Engineering and Automation, Northeastern University, Shenyang 110819, China;* orcid.org/0000-0003-0542-1739

Hong Liu − *State Key Laboratory of Drug Research, Shanghai Institute of Materia Medica, Chinese Academy of Sciences, Shanghai 201203, China;* orcid.org/0000-0003-3685-6268

Complete contact information is available at: https://pubs.acs.org/10.1021/acsomega.3c09983

Author Contributions

H.F. and G.L. contributed equally. H.H. conceived the research and designed the studies. H.F. performed most of the biological experiments and wrote the manuscript. G.L. performed bioinformatics analyses and visualization and was involved in the manuscript writing. L.L. performed the animal experiments under the supervision of H.L. X.R. performed the mass spectrometry analysis. Y.J., W.H., and K.L. were involved in the TPP experiments. R.L. provided advice for the biological experiments. H.H. supervised the study and revised the manuscript. All authors have approved the final version.

Notes

The authors declare no competing financial interest.

■ ACKNOWLEDGMENTS

This research was supported by the National Natural Science Foundation of China (22277125 and 92253306 to H.H.), the Natural Science Foundation of Shanghai (23ZR1474600 to H.H.), the Shandong Laboratory Program (SYS202205 to H.H.), and the Shanghai Municipal Science and Technology Major Project (to H.H.).

■ ABBREVIATIONS

ABCA1, ATP-binding cassette transporter A1; AGC, automatic gain control; BBR, berberine; CEACAM1, carcinoembryonic antigen-related cell adhesion molecule 1; CETSA, the cellular thermal shift assay; CVDs, cardiovascular diseases; DMEM, Dulbecco's modified Eagle's medium; GO, gene ontology; GSEA, gene set enrichment analysis; HDL, high-density lipoproteins; HFD, high diet feed; HLP, hyperlipoproteinemia; KEGG, Kyoto Encyclopedia of Genes and Genomes; LDL, low-density lipoprotein; LDLR, low-density lipoprotein receptor; LDL-C, low-density lipoprotein cholesterol; MI, myocardial infarction; NPC1, NPC intracellular cholesterol transporter 1; PCSK9, pro-protein convertase subtilisin-like/kexin type 9; PPIs, protein−protein interactions; SILAC, stable isotope labeling using amino acids in cell culture; TC, cholesterol; TG, triglyceride; TMT, tandem mass tag; TPP, thermal proteome profiling

■ REFERENCES

(1) Trinder, M.; Li, X.; DeCastro, M. L.; Cermakova, L.; Sadananda, S.; Jackson, L. M.; Azizi, H.; Mancini, G. J.; Francis, G. A.; Frohlich, J.; Brunham, L. R. Risk of premature atherosclerotic disease in patients with monogenic versus polygenic familial hypercholesterolemia. *J. Am. Coll. Cardiol.* **2019**, *74* (4), 512−522.

(2) Wang, C.; Pang, W.; Du, X.; Zhai, J.; Zhong, M.; Zhuang, M.; An, J.; Cao, L.; Zhang, L.; Zheng, W.; Zhang, J. Efficacy and safety of zhibitai in the treatment of hyperlipidemia: a systematic review and meta-analysis. *Front. Pharmacol.* **2022**, *13*, 974995.

(3) Wolf, D.; Ley, K. Immunity and inflammation in atherosclerosis. *Circ. Res.* **2019**, *124* (2), 315−327.

(4) Chen, K.; Ma, Z.; Yan, X.; Liu, J.; Xu, W.; Li, Y.; Dai, Y.; Zhang, Y.; Xiao, H. Investigation of the lipid-lowering mechanisms and active ingredients of Danhe granule on hyperlipidemia based on systems pharmacology. *Front. Pharmacol* **2020**, *11*, 528.

(5) Kruk, M. E.; Gage, A. D.; Joseph, N. T.; Danaei, G.; Garcia-Saiso, S.; Salomon, J. A. Mortality due to low-quality health systems in the universal health coverage era: a systematic analysis of amenable deaths in 137 countries. *Lancet* **2018**, *392* (10160), 2203−2212.

(6) Herrington, W.; Lacey, B.; Sherliker, P.; Armitage, J.; Lewington, S. Epidemiology of atherosclerosis and the potential to reduce the global burden of atherothrombotic disease. *Circ. Res.* **2016**, *118* (4), 535−546.

(7) Parihar, S. P.; Guler, R.; Brombacher, F. Statins: a viable candidate for host-directed therapy against infectious diseases. *Nat. Rev. Immunol.* **2019**, *19* (2), 104−117.

(8) Libby, P.; Buring, J. E.; Badimon, L.; Hansson, G. K.; Deanfield, J.; Bittencourt, M. S.; Tokgozoglu, L.; Lewis, E. F. Atherosclerosis. *Nat. Rev. Dis. Prim.* **2019**, *5* (1), 56.

(9) Grundy, S. M. Advances in treatment of dyslipidaemia. *Nat. Rev. Cardiol.* **2016**, *13* (2), 74−75.

(10) Sui, Y.; Zhao, H. L.; Wong, V. C.; Brown, N.; Li, X. L.; Kwan, A. K.; Hui, H. L.; Ziea, E. T.; Chan, J. C. A systematic review on use of Chinese medicine and acupuncture for treatment of obesity. *Obes. Rev.* **2012**, *13* (5), 409−430.

(11) Zhang, W. L.; Zhu, L.; Jiang, J. G. Active ingredients from natural botanicals in the treatment of obesity. *Obes. Rev.* **2014**, *15* (12), 957−967.

(12) Kang, Y. J.; Park, H.; Lee, Y.; Yoon, S.; Kwak, M. Sophora genomes provide insight into the evolution of alkaloid metabolites along with small-scale gene duplication. *BMC Genom.* **2023**, *24* (1), 475.
(13) You, L.; Yang, C.; Du, Y.; Wang, W.; Sun, M.; Liu, J.; Ma, B.; Pang, L.; Zeng, Y.; Zhang, Z.; Dong, X.; Yin, X.; Ni, J. A systematic review of the pharmacology, toxicology and pharmacokinetics of matrine. *Front. Pharmacol.* **2020**, *11*, 01067.
(14) Li, X.; Tang, Z.; Wen, L.; Jiang, C.; Feng, Q. Matrine: a review of its pharmacology, pharmacokinetics, toxicity, clinical application and preparation researches. *J. Ethnopharmacol.* **2021**, *269*, 113682.
(15) Zhang, H.; Chen, L.; Sun, X.; Yang, Q.; Wan, L.; Guo, C. Matrine: a promising natural product with various pharmacological activities. *Front. Pharmacol.* **2020**, *11*, 588.
(16) Gao, X.; Guo, S.; Zhang, S.; Liu, A.; Shi, L.; Zhang, Y. Matrine attenuates endoplasmic reticulum stress and mitochondrion dysfunction in nonalcoholic fatty liver disease by regulating SERCA pathway. *J. Transl. Med.* **2018**, *16* (1), 319.
(17) Li, C.; Xu, Y. H.; Hu, Y. T.; Zhou, X.; Huang, Z. S.; Ye, J. M.; Rao, Y. Matrine counteracts obesity in mice via inducing adipose thermogenesis by activating HSF1/PGC-1α axis. *Pharmacol. Res.* **2022**, *177*, 106136.
(18) Zhang, H. F.; Shi, L. J.; Song, G. Y.; Cai, Z. G.; Wang, C.; An, R. J. Protective effects of matrine against progression of high-fructose diet-induced steatohepatitis by enhancing antioxidant and anti-inflammatory defences involving Nrf2 translocation. *Food Chem. Toxicol.* **2013**, *55*, 70−77.
(19) Zhang, S.; Guo, S.; Gao, X. B.; Liu, A.; Jiang, W.; Chen, X.; Yang, P.; Liu, L. N.; Shi, L.; Zhang, Y. Matrine attenuates high-fat diet-induced in vivo and ox-LDL-induced in vitro vascular injury by regulating the PKCα/eNOS and PI3K/Akt/eNOS pathways. *J. Cell. Mol. Med.* **2019**, *23* (4), 2731−2743.
(20) Scully, T.; Ettela, A.; Kase, N.; LeRoith, D.; Gallagher, E. J. Unregulated LDL cholesterol uptake is detrimental to breast cancer cells. *Endocr. Relat. Cancer* **2023**, *30* (1), No. e220234.
(21) Yan, H.; Ma, Y. L.; Gui, Y. Z.; Wang, S. M.; Wang, X. B.; Gao, F.; Wang, Y. P. MG132, a proteasome inhibitor, enhances LDL uptake in HepG2 cells in vitro by regulating LDLR and PCSK9 expression. *Acta Pharmacol. Sin.* **2014**, *35* (8), 994−1004.
(22) Doncheva, N. T.; Morris, J. H.; Gorodkin, J.; Jensen, L. J. Cytoscape StringApp: network analysis and visualization of proteomics data. *J. Proteome Res.* **2019**, *18* (2), 623−632.
(23) Goncalves, A.; Roi, S.; Nowicki, M.; Dhaussy, A.; Huertas, A.; Amiot, M. J.; Reboul, E. Fat-soluble vitamin intestinal absorption: absorption sites in the intestine and interactions for absorption. *Food Chem.* **2015**, *172*, 155−160.
(24) Ouimet, M.; Barrett, T. J.; Fisher, E. A. HDL and reverse cholesterol transport. *Circ. Res.* **2019**, *124* (10), 1505−1518.
(25) Quazi, F.; Molday, R. S. Differential phospholipid substrates and directional transport by ATP-binding cassette proteins ABCA1, ABCA7, and ABCA4 and disease-causing mutants. *J. Biol. Chem.* **2013**, *288* (48), 34414−34426.
(26) Marcil, M.; Brooks-Wilson, A.; Clee, S. M.; Roomp, K.; Zhang, L. H.; Yu, L.; Collins, J. A.; van Dam, M.; Molhuizen, H. O.; Loubster, O.; Francis Ouellette, B.; Sensen, C. W.; Fichter, K.; Mott, S.; Denis, M.; Boucher, B.; Pimstone, S.; Genest, J., Jr.; Kastelein, J. J.; Hayden, M. R. Mutations in the ABC1 gene in familial HDL deficiency with defective cholesterol efflux. *Lancet* **1999**, *354* (9187), 1341−1346.
(27) Krimbou, L.; Denis, M.; Haidar, B.; Carrier, M.; Marcil, M.; Genest, J., Jr. Molecular interactions between apoE and ABCA1. *J. Lipid Res.* **2004**, *45* (5), 839−848.
(28) Najjar, S. M. Regulation of insulin action by CEACAM1. *Trends Endocrinol. Metab.* **2002**, *13* (6), 240−245.
(29) Al-Share, Q. Y.; DeAngelis, A. M.; Lester, S. G.; Bowman, T. A.; Ramakrishnan, S. K.; Abdallah, S. L.; Russo, L.; Patel, P. R.; Kaw, M. K.; Raphael, C. K.; Kim, A. J.; Heinrich, G.; Lee, A. D.; Kim, J. K.; Kulkarni, R. N.; Philbrick, W. M.; Najjar, S. M. Forced hepatic overexpression of CEACAM1 curtails diet-induced insulin resistance. *Diabetes* **2015**, *64* (8), 2780−2790.
(30) Heinrich, G.; Ghadieh, H. E.; Ghanem, S. S.; Muturi, H. T.; Rezaei, K.; Al-Share, Q. Y.; Bowman, T. A.; Zhang, D.; Garofalo, R. S.; Yin, L.; Najjar, S. M. Loss of hepatic CEACAM1: a unifying mechanism linking insulin resistance to obesity and non-alcoholic fatty liver disease. *Front. Endocrinol.* **2017**, *8*, 8.
(31) Yu, X. H.; Jiang, N.; Yao, P. B.; Zheng, X. L.; Cayabyab, F. S.; Tang, C. K. NPC1, intracellular cholesterol trafficking and atherosclerosis. *Clin. Chim. Acta* **2014**, *429*, 69−75.
(32) Colombo, A.; Dinkel, L.; Muller, S. A.; Sebastian Monasor, L.; Schifferer, M.; Cantuti-Castelvetri, L.; Konig, J.; Vidatic, L.; Bremova-Ertl, T.; Lieberman, A. P.; Hecimovic, S.; Simons, M.; Lichtenthaler, S. F.; Strupp, M.; Schneider, S. A.; Tahirovic, S. Loss of NPC1 enhances phagocytic uptake and impairs lipid trafficking in microglia. *Nat. Commun.* **2021**, *12* (1), 1158.
(33) Luo, J.; Yang, H.; Song, B. L. Mechanisms and regulation of cholesterol homeostasis. *Nat. Rev. Mol. Cell Biol.* **2020**, *21* (4), 225−245.
(34) Seidah, N. G.; Prat, A. The multifaceted biology of PCSK9. *Endocr. Rev.* **2022**, *43* (3), 558−582.
(35) Mineo, C. Lipoprotein receptor signalling in atherosclerosis. *Cardiovasc. Res.* **2020**, *116* (7), 1254−1274.
(36) Liu, Y.; Beyer, A.; Aebersold, R. On the dependency of cellular protein levels on mRNA abundance. *Cell* **2016**, *165* (3), 535−550.
(37) Sun, Y.; Xu, L.; Cai, Q.; Wang, M.; Wang, X.; Wang, S.; Ni, Z. Research progress on the pharmacological effects of matrine. *Front. Neurosci.* **2022**, *16*, 977374.
(38) Li, W.; Yu, X.; Tan, S.; Liu, W.; Zhou, L.; Liu, H. Oxymatrine inhibits non-small cell lung cancer via suppression of EGFR signaling pathway. *Cancer Med.* **2018**, *7* (1), 208−218.
(39) Merino Salvador, M.; Gomez de Cedron, M.; Moreno Rubio, J.; Falagan Martinez, S.; Sanchez Martinez, R.; Casado, E.; Ramirez de Molina, A.; Sereno, M. Lipid metabolism and lung cancer. *Crit. Rev. Oncol. Hematol.* **2017**, *112*, 31−40.
(40) Molina, D. M.; Jafari, R.; Ignatushchenko, M.; Seki, T.; Larsson, E. A.; Dan, C.; Sreekumar, L.; Cao, Y.; Nordlund, P. Monitoring drug target engagement in cells and tissues using the cellular thermal shift assay. *Science* **2013**, *341* (6141), 84−87.
(41) Jafari, R.; Almqvist, H.; Axelsson, H.; Ignatushchenko, M.; Lundback, T.; Nordlund, P.; Molina, D. M. The cellular thermal shift assay for evaluating drug target interactions in cells. *Nat. Protoc.* **2014**, *9* (9), 2100−2122.
(42) Savitski, M. M.; Reinhard, F. B.; Franken, H.; Werner, T.; Savitski, M. F.; Eberhard, D.; Molina, D. M.; Jafari, R.; Dovega, R. B.; Klaeger, S.; Kuster, B.; Nordlund, P.; Bantscheff, M.; Drewes, G. Tracking cancer drugs in living cells by thermal profiling of the proteome. *Science* **2014**, *346* (6205), 1255784.
(43) Ruan, C.; Ning, W.; Liu, Z.; Zhang, X.; Fang, Z.; Li, Y.; Dang, Y.; Xue, Y.; Ye, M. Precipitate-supported thermal proteome profiling coupled with deep learning for comprehensive screening of drug target proteins. *ACS Chem. Biol.* **2022**, *17* (1), 252−262.
(44) Mateus, A.; Kurzawa, N.; Becher, I.; Sridharan, S.; Helm, D.; Stein, F.; Typas, A.; Savitski, M. M. Thermal proteome profiling for interrogating protein interactions. *Mol. Syst. Biol.* **2020**, *16* (3), No. e9232.
(45) Cheng, W. W. L.; Budelier, M. M.; Sugasawa, Y.; Bergdoll, L.; Queralt-Martin, M.; Rosencrans, W.; Rostovtseva, T. K.; Chen, Z. W.; Abramson, J.; Krishnan, K.; Covey, D. F.; Whitelegge, J. P.; Evers, A. S. Multiple neurosteroid and cholesterol binding sites in voltage-dependent anion channel-1 determined by photo-affinity labeling. *Biochim. Biophys. Acta Mol. Cell Biol. Lipids* **2019**, *1864* (10), 1269−1279.
(46) Waterham, H. R.; Koster, J.; Romeijn, G. J.; Hennekam, R. C.; Vreken, P.; Andersson, H. C.; FitzPatrick, D. R.; Kelley, R. I.; Wanders, R. J. Mutations in the 3β-hydroxysterol Δ24-reductase gene cause desmosterolosis, an autosomal recessive disorder of cholesterol biosynthesis. *Am. J. Hum. Genet.* **2001**, *69* (4), 685−694.
(47) Shen, Y.; Zhou, J.; Nie, K.; Cheng, S.; Chen, Z.; Wang, W.; Wei, W.; Jiang, D.; Peng, Z.; Ren, Y.; Zhang, Y.; Fan, Q.; Richards, K. L.; Qi, Y.; Cheng, J.; Tam, W.; Ma, J. Oncogenic role of the SOX9-

https://doi.org/10.1021/acsomega.3c09983
ACS Omega 2024, 9, 24308−24320

DHCR24-cholesterol biosynthesis axis in IGH-BCL2+ diffuse large B-cell lymphomas. *Blood* **2022**, *139* (1), 73−86.
(48) Li, J.; Zhang, Y.; Qu, Z.; Ding, R.; Yin, X. ABCD3 is a prognostic biomarker for glioma and associated with immune infiltration: a study based on oncolysis of gliomas. *Front. Cell. Infect. Microbiol.* **2022**, *12*, 956801.
(49) Li, S.; Zeng, H.; Fan, J.; Wang, F.; Xu, C.; Li, Y.; Tu, J.; Nephew, K. P.; Long, X. Glutamine metabolism in breast cancer and possible therapeutic targets. *Biochem. Pharmacol.* **2023**, *210*, 115464.
(50) Yoo, H. C.; Yu, Y. C.; Sung, Y.; Han, J. M. Glutamine reliance in cell metabolism. *Exp. Mol. Med.* **2020**, *52* (9), 1496−1516.
(51) Wang, K.; Ye, X.; Yin, C.; Ren, Q.; Chen, Y.; Qin, X.; Duan, C.; Lu, A.; Gao, L.; Guan, D. Computational metabolomics reveals the potential mechanism of matrine mediated metabolic network against hepatocellular carcinoma. *Front. Cell Dev. Biol.* **2022**, *10*, 859236.
(52) Rao, S. W.; Duan, Y. Y.; Zhao, D. S.; Liu, C. J.; Xu, S. H.; Liang, D.; Zhang, F. X.; Shi, W. Integrative analysis of transcriptomic and metabolomic data for identification of pathways related to matrine-induced hepatotoxicity. *Chem. Res. Toxicol.* **2022**, *35* (12), 2271−2284.
(53) Ference, B. A.; Ginsberg, H. N.; Graham, I.; Ray, K. K.; Packard, C. J.; Bruckert, E.; Hegele, R. A.; Krauss, R. M.; Raal, F. J.; Schunkert, H.; Watts, G. F.; Boren, J.; Fazio, S.; Horton, J. D.; Masana, L.; Nicholls, S. J.; Nordestgaard, B. G.; van de Sluis, B.; Taskinen, M. R.; Tokgozoglu, L.; Landmesser, U.; Laufs, U.; Wiklund, O.; Stock, J. K.; Chapman, M. J.; Catapano, A. L. Low-density lipoproteins cause atherosclerotic cardiovascular disease. 1. Evidence from genetic, epidemiologic, and clinical studies. A consensus statement from the European Atherosclerosis Society Consensus Panel. *Eur. Heart J.* **2017**, *38* (32), 2459−2472.
(54) Wang, J.; Zhao, J.; Yan, C.; Xi, C.; Wu, C.; Zhao, J.; Li, F.; Ding, Y.; Zhang, R.; Qi, S.; Li, X.; Liu, C.; Hou, W.; Chen, H.; Wang, Y.; Wu, D.; Chen, K.; Jiang, H.; Huang, H.; Liu, H. Identification and evaluation of a lipid-lowering small compound in preclinical models and in a Phase I trial. *Cell Metab.* **2022**, *34* (5), 667−680 e6.
(55) Khan, S. U.; Yedlapati, S. H.; Lone, A. N.; Hao, Q.; Guyatt, G.; Delvaux, N.; Bekkering, G. E. T.; Vandvik, P. O.; Riaz, I. B.; Li, S.; Aertgeerts, B.; Rodondi, N. PCSK9 inhibitors and ezetimibe with or without statin therapy for cardiovascular risk reduction: a systematic review and network meta-analysis. *BMJ* **2022**, *377*, No. e069116.
(56) Giugliano, R. P.; Cannon, C. P.; Blazing, M. A.; Nicolau, J. C.; Corbalan, R.; Špinar, J.; Park, J.-G.; White, J. A.; Bohula, E. A.; Braunwald, E. Benefit of adding ezetimibe to statin therapy on cardiovascular outcomes and safety in patients with versus without diabetes mellitus. *Circulation* **2018**, *137* (15), 1571−1582.

https://doi.org/10.1021/acsomega.3c09983
ACS Omega 2024, 9, 24308−24320